PHYSICAL REVIEW B VOLUME 38, NUMBER 8 15 SEPTEMBER 1988-I

Theoretical study of the electronic structure of ordered and disordered Cu_3Au

P. Weinberger
Institut für Technische Elektrochemie, Technical University Vienna, Austria
and Center of Materials Science, Los Alamos National Laboratory, Los Alamos, New Mexico 87545

A. M. Boring and R. C. Albers
Los Alamos National Laboratory, Los Alamos, New Mexico 87545

W. M. Temmerman
Science and Engineering Research Council, Daresbury Laboratory, Daresbury, United Kingdom

(Received 13 October 1987; revised manuscript received 4 April 1988)

The electronic structure of the ordered phase of Cu_3Au is investigated using the self-consistent-field (SCF) fully relativistic linear-muffin-tin-orbital method. The electronic structure of the disordered phase is obtained from a fully relativistic Korringa-Kohn-Rostoker coherent-potential-approximation calculation. To show the effects of self-consistency in the disordered phase, we present both non-SCF and SCF results for this phase. These results show that the largest changes in the electronic structure upon ordering are in energy regions away from the Fermi energy. To verify this prediction we have calculated the x-ray-photoemission (XPS) intensities for both phases and compared these to experimental data. It is found that the calculated Al $K\alpha$ XPS intensity is in excellent agreement with the data on the ordered system and gives a clear picture of the itinerant nature of the Au 5*d* states. For the disordered state our results are in agreement with trends seen in angle-resolved photoemission, but are in disagreement with the only angle-integrated XPS data available on the disordered system.

I. INTRODUCTION

Although the order-disorder phase transition in the Cu_3Au system is probably one of the oldest transitions considered by the metallurgical community it is still not well understood. First, the Fermi surface of the ordered state obtained from de Haas–van Alphen data[1] has been interpreted as an indication of a strong electronic contribution to the order-disorder transformation. On the other hand, Lander *et al.*[2,3] have interpreted their neutron-diffraction data as indicating that phonon anomalies may be responsible for the transition. There does seem to be agreement, however, that the changes in electronic structure between the ordered and disordered state near the Fermi energy (E_F) are small and subtle.

If one does not focus on the transition and the states near E_F, but looks at the electronic states away from E_F in the two phases, larger changes are seen. There have been several photoemission studies[4,5] of the ordered phase which are in good agreement with one another, but which give different interpretations to their data. First, Eberhardt *et al.*[4] interprets the spin-orbit splitting of the Au *d* states as an indication that these states are localized. DiCenzo *et al.* maintain that their x-ray-photoemission (XPS) data is consistent with an itinerant picture of these Au states. For the disordered phase the two available photoemission studies[6,7] agree in that they both show that the large changes in electronic structure upon disordering occur in Au 5*d* states (several eV below E_F). However, one study indicates that the Au 5*d* become featureless upon disordering[6] while the other[7] shows the lowest Au peak growing and becoming sharper upon disordering.

The electronic structure of the ordered Cu_3Au phase appears to be reasonably well understood. The de Haas–van Alphen measurements (Deimel *et al.*[1]) are found to be in good agreement with corresponding band-structure results (Skriver and Lengkeek[8]) obtained in terms of the linear-muffin-tin-orbital (LMTO) method with mass-velocity and Darwin corrections.[9] However, because that was a non-self-consistent calculation certain features of the electronic structure may be expected to be missing. This is seen most clearly in the comparison of their density-of-states (DOS) functions[8] with the photoemission data of Nemoshkalenko *et al.*[7] in which their gold bands have to be shifted by 0.4 eV relative to their copper bands in order to obtain a rough correlation with the data.[7] Since matrix elements were not calculated theirs was really only a crude comparison. At this point it is hard to know whether the lack of agreement to the XPS data is due to a lack of self-consistency or is due to the constant-matrix-element approximation. To answer these questions we have performed a fully relativistic self-consistent LMTO calculation[10] for the ordered phase of Cu_3Au. In order to compare with the XPS data we have calculated the photoemission matrix elements,[11] so we obtain theoretical XPS intensities.

The electronic structure in the disordered phase is even less well studied and less well understood. This is unfortunate for it is precisely the electronic structure in the disordered state that enters into the theory of compositional disorder (Gyorffy and Stocks[12]), which is one of the most striking phenomena displayed by this alloy system (Clapp and Moss,[13] Hashimoto and Ogawa,[14] Moss and Walker,[15] Zhu and Cowley[16]).

As mentioned before in the present work the fully relativistic (solutions to the Dirac equation) LMTO method[10] is applied for the ordered phase, whereas for the disordered state the fully relativistic Korringa-Kohn-Rostoker coherent-potential approximation (RKKR-CPA, Staunton *et al.*[17]) is used. For the disordered state two separate calculations are performed, namely, (1) a non-self-consistent-field (non-SCF) RKKR-CPA calculation based on self-consistent muffin-tin LMTO potentials for the ordered system and (2) a self-consistent RKKR-CPA calculation. The reason for including the non-self-consistent results is to show the effects of self-consistency in the RKKR-CPA method as most results in the literature are of the non-self-consistent variety. Finally having obtained the DOS functions from these calculations, we then calculate the XPS intensities[11] and compare them to the existing data.[4-6]

II. PRACTICAL AND NUMERICAL ASPECTS

The ordered-phase calculations were performed self-consistently using the fully relativistic linear-muffin-tin-orbital (LMTO) method[10] within the local-density approximation. Calculations were performed using both the Kohn-Sham exchange-only potential and the Barth-Hedin exchange-correlation potential[18] to check the sensitivity of the results to the potential approximation used. It was found that the quantities reported in this paper such as densities of states (DOS) and photoemission intensities (XPS) were insensitive to the potential approximation. The results presented here are for the Barth-Hedin[18] approximation. The calculations were, of course, performed for the Cu_3Au crystal structure at the experimental lattice constant of 3.7478 Å. For this crystal structure, the band structure was converged for 95 k points in the irreducible wedge of the Brillouin zone (BZ) within the atomic-sphere approximation (ASA). The tetrahedron method[19] was used to obtain the DOS functions. The core states were taken from atomic Dirac calculations and were held fixed throughout the self-consistent-field cycles of the band electrons.

In the case of the non-SCF RKKR-CPA calculations, the Cu and Au scattering potentials correspond to self-consistent LMTO potentials for the ordered systems. For the LMTO calculations the common muffin-tin zero corresponded to the mean value of the scattering potentials at the muffin-tin radius. For the BZ integration the 21 directions of Fehlner and Vosko[20] are used and the SCF scattering amplitudes are calculated at real energies.

In the fully SCF RKKR-CPA calculation a frozen-core approximation was also applied. It should be noted that a SCF RKKR-CPA calculation involves two self-consistency cycles, one for the scattering amplitudes (this solves the problem of averaging over all compositional configurations), and another for the charge densities as required by the density-functional theory. This implies that for each step in the self-consistency cycle for the charge densities a self-consistency cycle for the scattering amplitudes has to be carried out. The muffin-tin charge densities are obtained by an energy integration of the Green's function along a rectangular contour in the complex plane, similar to the nonrelativistic case as described by Johnson *et al.*[21] and Pinski and Stocks.[22] This contour passes the real axis below the bottom of the valence s band and at the Fermi energy. The Coulomb part of the potential is found by solving Poisson's equation, the constant potential refers to a concentration-averaged constant charge density in the region between the muffin-tin spheres. Contrary to a calculation for an ordered system no Madelung term is involved (for a more formal description of the self-consistency procedure see, for example, Weinberger and Gonis[23]).

The scattering potentials (i.e., the charge densities for the components Cu and Au) are iterated until the individual fcc band structures for Cu and Au change by less than about 1 mRy in two subsequent iterations using the corresponding potentials in Cu_3Au and the Cu_3Au lattice constant. This rough convergence criterion yields a convergence of the d-like resonance energies (the energy at which the corresponding phase shift passes through $\pi/2$) of about 1–2 mRy. Throughout the total self-consistency procedure including the final iteration the BZ integrations are performed using the five special directions of Bansil.[24]

For the SCF potentials the CPA scattering amplitudes are calculated in the complex plane parallel to the real axis in steps of 0.002 d.u. [1 d.u. $=(a^2/4\pi^2$ Ry), where a is the lattice constant] and are numerically continued (Pindor *et al.*[25] and Klima *et al.*[26]) to the real axis by means of the Riemann-Cauchy condition. Because of this numerical procedure a small imaginary part to the energy parameter remains, causing some artificial broadening of the density-of-states functions. For the calculation of the electronic structure of the disordered phase the local-density-functional approximation of Barth and Hedin is also applied.

The x-ray photoemission spectra (XPS) intensities were calculated as outlined previously.[11] Here just a description of the main points is given. The starting point is the one-electron formulation of Feibelman and Eastman[27] which contains the electron-photon interaction, the initial-state Green's function, and the time-reversed low-energy electron-diffraction (LEED) function. For the high photon energies of XPS the fully relativistic angle-integrated intensity $I(E+\omega)$ can be expressed as

$$I(E+\omega)=\sum_{i(\text{sites})}\sum_{\kappa}\sigma_{\kappa}^{i}(E+\omega)n_{\kappa}^{i}(E)\ .$$

In this expression the $n_{\kappa}^{i}(E)$ are the partial DOS functions for the κth (relativistic quantum number) channel on the ith site and $\sigma_{\kappa}^{i}(E+\omega)$ are the relativistic cross sections calculated over the energy range of the DOS functions for fixed incident photon energy ($\omega=1486.6$ eV for the Al $K\alpha$ line). This expression shows that for the high energies of XPS the connection between the intensity I and the intrinsic electronic structure represented by the DOS function $n_{\kappa}^{i}(E)$ is a simple one.

III. RESULTS

A. Densities of states

In Fig. 1 the density of states of the ordered calculation is compared with the two disordered calculations. In Figs. 1(b) and 1(c) also the concentration weighted component DOS are shown whereas in Fig. 1(a) only the Au-like density of states is marked separately. We will discuss the DOS for the ordered state and then compare it to the results for the two disordered-phase calculations. First, we could not really compare our results to those of Skriver and Lengkeek because their figure (see Ref. 8) is just too small. Therefore, we can only give their description of their results and compare that with our fully relativistic self-consistent results. Their overall *d* bands (Cu and Au) are 5.5 eV wide with the top of the Cu bands 1.8 eV below E_F. This is in reasonable agreement with our SCF results in which the top of the Cu bands is 1.7 eV below E_F and the overall width (Cu and Au bands) is 5.1 eV. This also indicates that their Cu and Au bandwidths are individually correct (in agreement with ours) and their assessment that their Au bands are too low by 0.4 eV is correct also. From our results a few more details of the electronic structure can be given. Our Cu bands are 2.3 eV wide and our Au bands are 2.8 eV wide. Comparing these results to the electronic structure of the pure metals we note that in Cu_3Au the Cu *d* bands are the same width as in pure Cu and in the same position relative to E_F (1.7 eV below). Of course, it is reasonable that the Cu bands would be the least disturbed by replacing every fourth Cu atom by a Au atom.

For the disordered case, we see that in both the non-SCF (b) and the SCF (c) calculation, the structure seen in the Au part of the DOS of the ordered state is completely washed out. For the Cu *d* states the non-SCF calculation still has some structure whereas the SCF results yield a fairly smooth DOS function. As mentioned above, part of this difference is due to the extra broadening in the SCF calculation. The width of the Cu *d* band, however, is about the same in both calculations and the first Cu peak below E_F is also in the same position. The Au *d* states are also very similar below -5 eV, but have less structure in the region of the Cu *d* bands in the SCF results. Also we note that the separation between Au *d* and Cu *d* states seen in the ordered calculation is not seen in the non-SCF result, but seems to reappear in the SCF calculations. At the present time we have no simple explanation for this hybridizationlike gap in the SCF result. In comparing the ordered DOS with the disordered DOS it is seen that the Cu *d* bandwidth is only slightly broadened (about 0.3 eV) upon disordering. The Au *d* band states, on the other hand, undergo considerable broadening (over 1.0 eV) upon disordering. Also the two large peaks (at 5.5 and 6.6 eV below E_F) seen in the ordered state, which we will show are due to spin-orbit splitting, are completely washed out in the disordered phase.

B. X-ray-photoemission spectra

In Fig. 2 the calculated *d*-like Al $K\alpha$ photoemission cross sections are shown for Au and Cu in the case of or-

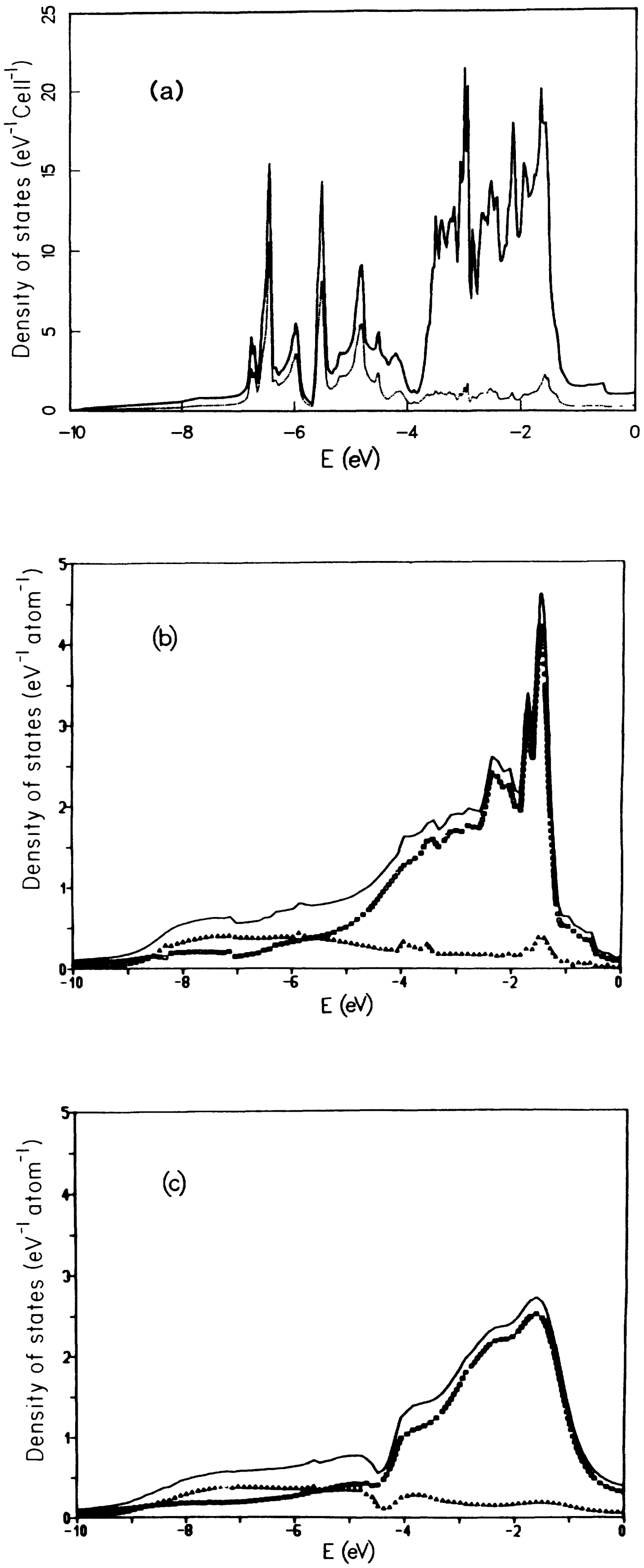

FIG. 1. (a) Density of states for ordered Cu_3Au for the total (solid line) and Au component (dotted line). (b) Non-SCF density of states for disordered Cu_3Au for the total (solid line), the Cu component (squares), and Au component (triangles). (c) SCF density of states for disordered Cu_3Au for the total (solid line), Cu component (squares), and Au component (triangles).

dered Cu_3Au. Note that the *d*-like cross sections of Au are larger by a factor of 3 than those of Cu, which in turn implies that the Au-like contribution to the total intensity will be much bigger than suggested by the density of states in Fig. 1(a). The reason the Au cross sections are larger is simple: the cross sections are proportional to the average of r^2 over the orbitals in question and the Au 5*d* orbitals are quite a bit larger in radial extent than the Cu 3*d* orbitals (see also the discussion in Ref. 28).

In Fig. 3 the most recent experimental Al $K\alpha$ photoemission spectrum[5] for ordered Cu_3Au [Fig. 3(a)] is compared with our calculated Al $K\alpha$ XPS intensities for the ordered phase [Fig. 3(b)]. The theoretical spectra include a spectrometer resolution of 0.6 eV and a quadratic lifetime broadening with a half-width of 1 eV at the band bottom for the ordered state. The experimental spectrum shows three well-defined peaks, namely at about −7.0, −5.5, and −2.5 eV, with a shoulder on the high-energy peak at about −3.8 eV. Our theoretical intensity seems to map these peaks very nicely, except that the peak positions are shifted by 0.7 eV towards higher energies *and* there is a double peak at −4.8 and −5.5 eV. If we shift our theoretical spectra by this 0.7 eV we obtain almost perfect agreement for both peak positions and widths for both Cu and Au states. The two-peak structure seen experimentally in the Au states will be shown (below) to be due to spin-orbit splitting in these itinerant states. Also the shoulder on the Cu peak at −3.8 eV is well reproduced in the calculations.

The theoretical spectrum for the disordered phase (Fig. 4), which is based upon the SCF RKKR-CPA calculation, shows the main Cu peak at −1.7 eV. This is exactly where the corresponding peak in the theoretical spectrum for the ordered phase is located. All other features, "washed out" because of disorder, are in the vicinity where there are the low-energy peaks in the experimental

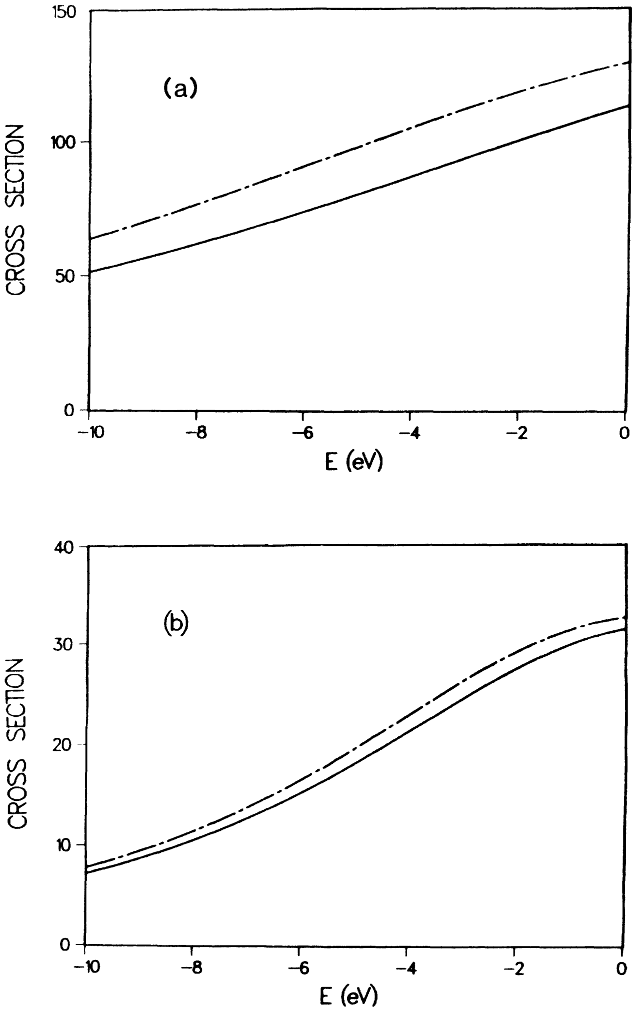

FIG. 2. Partial *d*-like Al $K\alpha$ photoemission cross sections (arbitrary units) for (a) Au and (b) Cu in ordered Cu_3Au. The $d^{3/2}$-like cross sections are shown as dashed-dotted lines, the $d^{5/2}$-like cross sections as solid lines.

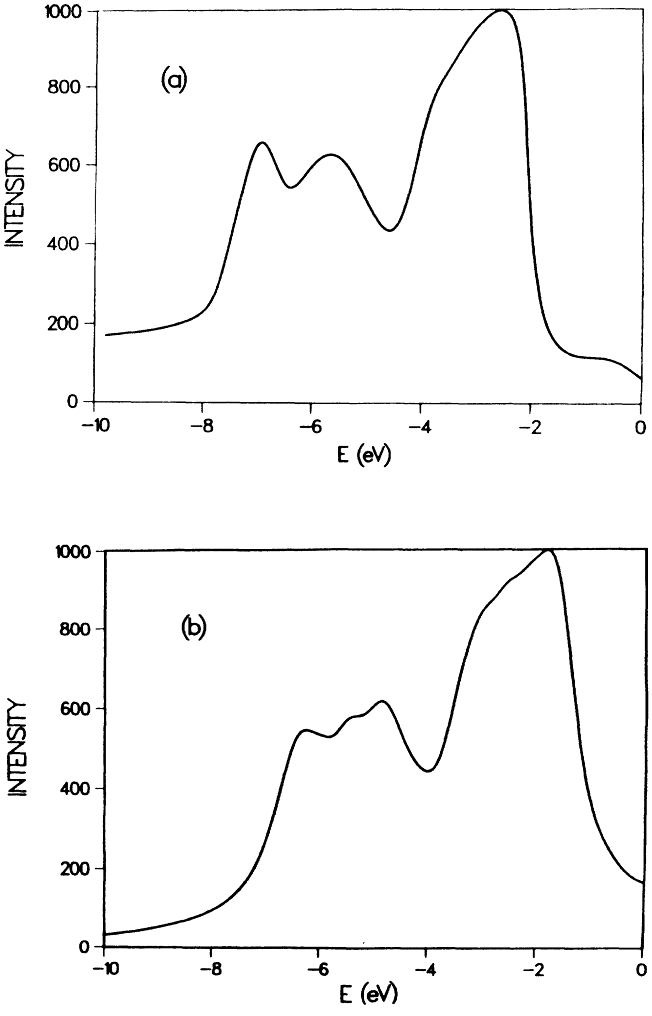

FIG. 3. (a) Experimental Al $K\alpha$ photoemission spectrum (arbitrary units) for ordered Cu_3Au [data from DiCenzo *et al.* (Ref. 5)]. (b) Theoretical Al $K\alpha$ photoemission spectrum (arbitrary units) for ordered Cu_3Au.

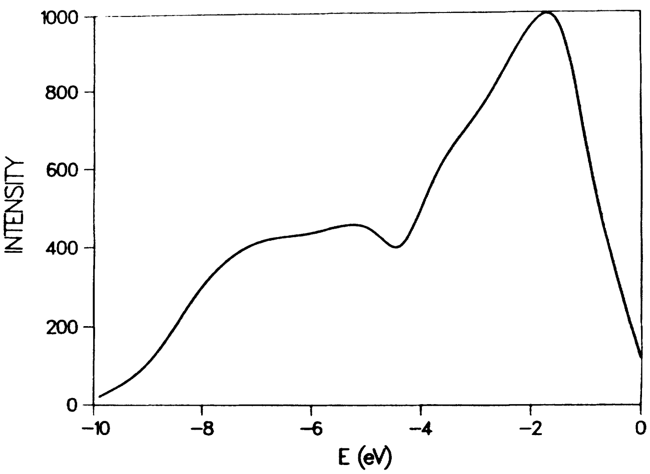

FIG. 4. Theoretical Al $K\alpha$ photoemission spectrum (arbitrary units) for disordered Cu_3Au.

spectrum of the ordered phase.[5] A comparison between theory and experiment for the disordered phase is rather difficult at this time. The only XPS data on the disordered phase are those of Nemoshkalenko *et al.*,[7] which are questionable because their spectra for the ordered phase disagree (1 eV narrower) with all the other corresponding photoemission studies. Their data show the lowest Au peak becoming larger and sharper upon disordering in contrast to our results and in contrast to the experimental results of Jordan *et al.*[6] for angle-resolved photoemission. While we cannot compare our results directly with these angle-resolved data,[6] we agree with the smearing out of features in the Au states upon disordering.

In order to understand the various features in the experimental spectrum for ordered Cu_3Au in Fig. 3, the d-like contributions of Au and Cu states to the total intensity are shown. Now a satisfactory interpretation of the experimental data is at hand [and also the reason why in Fig. 3(b) the spectrometer resolution is chosen to be relatively small]: the two lower-energy peaks in Fig. 3(a) are due to the spin-orbit splitting of the Au d bands, and the asymmetry of the experimental peak at -5.5 eV is caused by the double-peak structure at -5.5 and -4.8 eV in Fig. 3(b). A larger spectrometer resolution makes these two peaks collapse into one. The shoulder in the experimental XPS at about -3.8 eV can clearly be seen from Fig. 5 to be caused by hybridization of Cu $d^{3/2}$-like states with the Au-like states. The dominant peak in the experimental spectrum, the peak at $\simeq -2.5$ eV, arises mostly from Cu $d^{5/2}$-like states, however, with considerably large contributions from Cu $d^{3/2}$-like and Au d-like states.

IV. CONCLUSION

The theoretical x-ray-photoemission spectrum for the ordered phase which is based on a fully relativistic LMTO calculation, can explain the shape of the experimental spectrum very well. However, as far as peak positions are concerned, shifts of at least 0.7 eV have to be made to obtain this agreement. This should be kept in mind when comparing theoretical with experimental angle-resolved photoemission results either for the ordered or the disordered state of Cu_3Au. One conclusion that can be drawn from our calculations is that the changes in the electronic structure in the ordered and disordered phases are largest for the Au d states which are not near the Fermi energy. Because we have given a detailed comparison for the ordered state and get excellent agreement with the XPS data, it would be nice to have our predictions for the disordered state checked by a careful experimental XPS study.

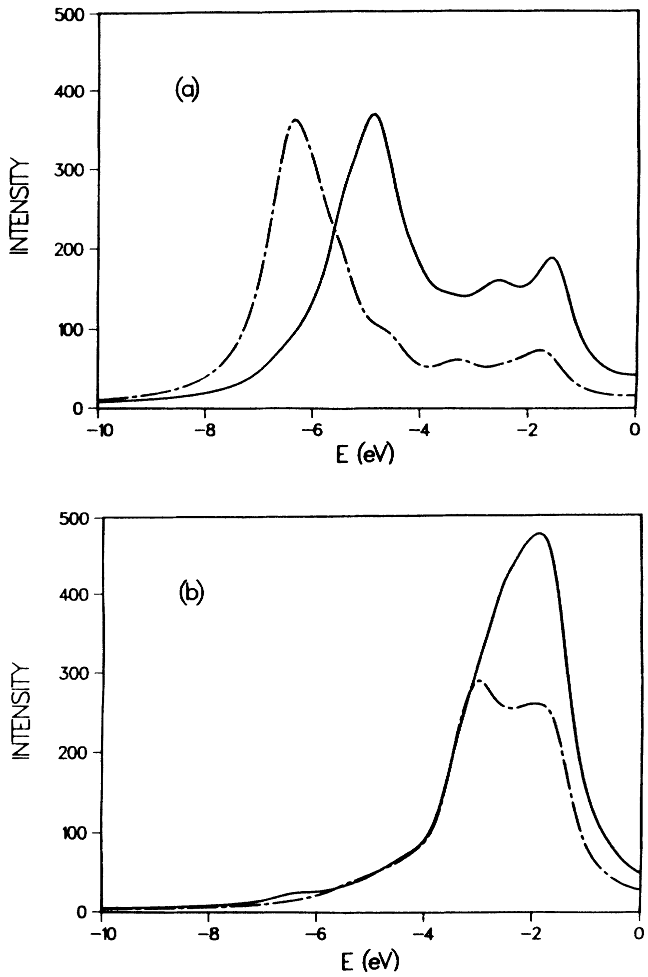

FIG. 5. Partial d-like contributions of (a) Au and (b) Cu to the total intensity (arbitrary units). The $d^{3/2}$-like contributions are shown as dashed-dotted lines, the $d^{5/2}$-like contributions as solid lines for the ordered case.

ACKNOWLEDGMENTS

The authors are most grateful to Dr. B. L. Gyorffy for many discussions and comments. One of us (P.W.) wishes to acknowledge financial support by the Jubiläumsstiftung der Stadt Wien.

[1] P. P. Deimel, R. J. Higgins, and R. K. Goodall, Phys. Rev. B **24**, 6197 (1981).

[2] G. H. Lander, P. J. Brown, and J. Faber, Jr., J. Phys. C **15**, 6699 (1982).

[3] G. H. Lander and P. J. Brown, J. Phys. C **18**, 2017 (1985).

[4] W. Eberhardt, S. C. Wu, R. Garrett, D. Sondericker, and F. Jona, Phys. Rev. B **31**, 8285 (1985).

[5] S. B. Di Cenzo, P. H. Citrin, E. H. Hartford, Jr., and C. K. Wertheim, Phys. Rev. B **34**, 1343 (1986).

[6] R. G. Jordan, G. S. Sohal, B. L. Gyorffy, P. J. Durham, W. M. Temmerman, and P. Weinberger, J. Phys. F **15**, L135 (1985).

[7] V. V. Nemoshkalenko, K. V. Chuistov, V. G. Aleshin, and A. I. Senkevich, J. Electron Spectrosc. Relat. Phenom. **9**, 169 (1976).

[8] H. L. Skriver and H. P. Lengkeek, Phys. Rev. **19**, 900 (1979). This paper gave semirelativistic results both with and without spin-orbit coupling, and we could not determine from the paper how their non-SCF results with spin-orbit coupling were obtained.

[9] O. K. Andersen, Phys. Rev. B **12**, 3060 (1975); H. L. Skriver, *The LMTO Method* (Springer, Berlin, 1984); N. E. Christensen, Int. J. Quantum Chem. **25**, 233 (1984).

[10] N. E. Christensen, J. Phys. F **8**, L51 (1978); Int. J. Quantum Chem. **25**, 233 (1984).

[11] P. Marksteiner, P. Weinberger, R. C. Albers, A. M. Boring, and G. Schadler, Phys. Rev. B **34**, 6730 (1986).

[12] B. L. Gyorffy and G. M. Stocks, Phys. Rev. Lett. **50**, 374 (1983).

[13] P. C. Clapp and S. C. Moss, Phys. Rev. **171**, 754 (1968).

[14] S. Hashimoto and S. Ogawa, J. Phys. Soc. Jpn. **29**, 710 (1970).

[15] S. C. Moss and R. H. Walker, J. Appl. Crystallogr. **8**, 96 (1974).

[16] J. Zhu and J. M. Cowley, Acta Crystallogr. A **38**, 718 (1982).

[17] S. Staunton, B. L. Gyorffy, and P. Weinberger, J. Phys. F **10**, 2665 (1980).

[18] U. von Barth and L. Hedin, J. Phys. C **5**, 1629 (1972).

[19] G. Lehman and M. Taut, Phys. Status Solidi **54**, 469 (1972).

[20] H. Fehlner and S. H. Vosko, Can. J. Phys. **54**, 2159 (1976).

[21] D. D. Johnson, F. J. Pinski, and G. M. Stocks, Phys. Rev. B **30**, 5508 (1984).

[22] F. J. Pinski and G. M. Stocks, Phys. Rev. B **32**, 4204 (1985).

[23] P. Weinberger and A. Gonis, in *Handbook on the Physics and Chemistry of the Actinides,* edited by A. J. Freeman, C. Keller, and G. H. Lander (North-Holland, Amsterdam, 1986).

[24] A. Bansil, Solid State Commun. **16**, 885 (1975).

[25] A. J. Pindor, W. N. Temmerman, and B. L. Gyorffy, J. Phys. F **12**, 1627 (1983).

[26] J. Klima, G. Schadler, P. Weinberger, and A. Neckel, J. Phys. F **15**, 1307 (1985).

[27] P. J. Feibelman and D. E. Eastman, Phys. Rev. B **10**, 4932 (1974).

[28] U. Konig, P. Marksteiner, J. Redinger, P. Weinberger, and H. Ebert, Z. Phys. B **65**, 139 (1986).